Suppressor screening reveals common kleisin–hinge interaction in condensin and cohesin, but different modes of regulation

Xingya Xu[a] and Mitsuhiro Yanagida[a,1]

[a]G0 Cell Unit, Okinawa Institute of Science and Technology Graduate University, Onna-son, 904-0495 Okinawa, Japan

Contributed by Mitsuhiro Yanagida, April 1, 2019 (sent for review February 15, 2019; reviewed by Kerry Bloom, David M. Glover, and Robert V. Skibbens)

Cohesin and condensin play fundamental roles in sister chromatid cohesion and chromosome segregation, respectively. Both consist of heterodimeric structural maintenance of chromosomes (SMC) subunits, which possess a head (containing ATPase) and a hinge, intervened by long coiled coils. Non-SMC subunits (Cnd1, Cnd2, and Cnd3 for condensin; Rad21, Psc3, and Mis4 for cohesin) bind to the SMC heads. Here, we report a large number of spontaneous extragenic suppressors for fission yeast condensin and cohesin mutants, and their sites were determined by whole-genome sequencing. Mutants of condensin's non-SMC subunits were rescued by impairing the SUMOylation pathway. Indeed, SUMOylation of Cnd2, Cnd3, and Cut3 occurs in midmitosis, and Cnd3 K870 SUMOylation functionally opposes Cnd subunits. In contrast, cohesin mutants *rad21* and *psc3* were rescued by loss of the RNA elimination pathway (Erh1, Mmi1, and Red1), and loader mutant *mis4* was rescued by loss of Hrp1-mediated chromatin remodeling. In addition, distinct regulations were discovered for condensin and cohesin hinge mutants. Mutations in the N-terminal helix bundle [containing a helix–turn–helix (HTH) motif] of kleisin subunits (Cnd2 and Rad21) rescue virtually identical hinge interface mutations in cohesin and condensin, respectively. These mutations may regulate kleisin's interaction with the coiled coil at the SMC head, thereby revealing a common, but previously unknown, suppression mechanism between the hinge and the kleisin N domain, which is required for successful chromosome segregation. We propose that in both condensin and cohesin, the head (or kleisin) and hinge may interact and collaboratively regulate the resulting coiled coils to hold and release chromosomal DNAs.

SMC head | SMC hinge | kleisin | SUMO | RNA elimination

Isolation of extragenic suppressors is a convenient tool to search for genes with protein products that function in the same process as a gene of interest, or that physically interact with that gene's protein product (1–4). Alternatively, extragenic suppressors often oppose the gene function that is impaired. For example, the loss of adenylate cyclase (resulting in reduced cAMP concentration) is compensated for by mutations in phosphodiesterase, which cause an increase in [cAMP] (5, 6). We previously developed an efficient and cost-effective suppressor mutation identification method using next-generation sequencing of a genomic DNA mixture to identify suppressor mutations produced spontaneously under restrictive conditions (7). The initial mutation is temperature-sensitive (ts), causing, for example, protein instability, and the extragenic suppressor mutation (the second mutation) can alleviate or cover the ts phenotype by stabilizing the protein or protein–protein interactions. For example, ts histone H2B mutant *htb1-G52D* fails to form colonies at 36 °C, and multiple *htb1-G52D* suppressors were identified in Spt-Ada-Gcn5-acetyl transferase (SAGA) complex genes (e.g., *ubp8*, *gcn5*) using the method (7). The SAGA complex contains deubiquitinating activity of histone H2B, which deubiquitinates and destabilizes H2B. Hence, Δ*ubp8* and Δ*gcn5* stabilized H2B and were able to rescue the ts phenotype. Two other examples of genetic suppression involving Cdc48-mediated proteasome-dependent destruction and the Eso1-Wpl1–mediated cohesion establishment/dissolution cycle have been demonstrated (7). This kind of approach, if employed systematically using numerous mutations, can be developed on a much more comprehensive scale, and will give us a systematic view of how complex molecular assemblies are organized (8).

Condensin and cohesin are two fundamental protein complexes required to generate functional chromosome structure. Both contain structural maintenance of chromosomes (SMC) subunits, which are composed of three domains, namely, the head, coiled coil, and hinge. Each SMC subunit comprises two head segments at the N and C termini, a hinge segment in the middle, and two 50-nm coiled coils linking the head and hinge segments (9, 10) (Fig. 1*A*). Condensin and cohesin contain additional essential subunits. In the fission yeast *Schizosaccharomyces pombe*, in addition to the heterodimeric Cut14/SMC2 and Cut3/SMC4 (11–13), three subunits are bound to the head region of condensin (Cnd1/NCAPD2, Cnd2/NCAPH, and Cnd3/NCAPG; NCAPD2, NCAPH, and NCAPG are their human homologs) (14, 15). For cohesin, heterodimeric Psm1/SMC1 and Psm3/SMC3 head domains associate with Rad21/RAD21, Psc3/STAG1–3, and Mis4/NIPBL subunits (RAD21, STAG1–3, NIPBL are their human homologs) (16, 17). SMC heads have ATPase activity

Significance

Condensin and cohesin are heteropentameric complexes containing two structural maintenance of chromosomes (SMC) subunits and three non-SMC subunits. SMC dimers form head and hinge domains connected by long coiled coils. Suppressor screening for head-associated non-SMC, and SMC hinge mutants of fission yeast, reveals that condensin is regulated by SUMOylation, ubiquitination, and phosphorylation, while cohesin is regulated by RNA elimination and chromatin remodeling and releasing factors. So, they are regulated by distinct pathways. However, hinge interface mutations are commonly suppressed by mutations in the kleisin N terminus. The results support a "hold and release" model, in which the head and hinge interact to form arched coiled coils that hold and release chromosomal DNAs. The head-kleisin and hinge may cooperate to regulate arched coiled coils' orientation, which affects their interaction with DNAs.

Author contributions: X.X. and M.Y. designed research; X.X. performed research; X.X. and M.Y. analyzed data; and X.X. and M.Y. wrote the paper.

Reviewers: K.B., University of North Carolina at Chapel Hill; D.M.G., University of Cambridge; and R.V.S., Lehigh University.

The authors declare no conflict of interest.

Data deposition: The sequencing data reported in this paper have been deposited in the National Center for Biotechnology Information BioProject database (accession nos. PRJNA450289 and PRJNA525996).

[1]To whom correspondence should be addressed. Email: myanagid@gmail.com.

This article contains supporting information online at www.pnas.org/lookup/suppl/doi:10.1073/pnas.1902699116/-/DCSupplemental.

Published online May 9, 2019.

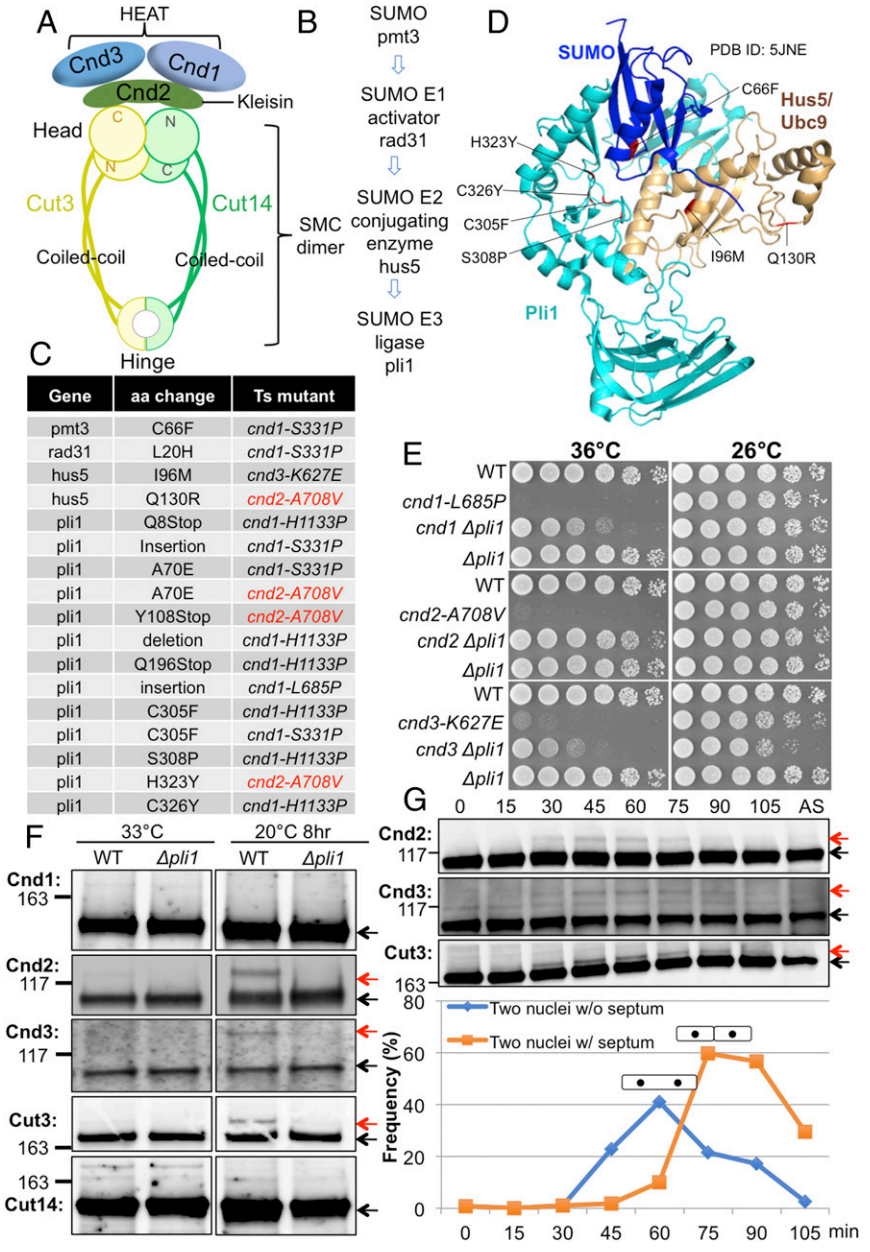

Fig. 1. Loss of SUMOylation suppresses ts *cnd1*, *cnd2*, and *cnd3* mutations. (*A*) Arrangement of the subunits in the fission yeast condensin complex. Cut3/SMC4 and Cut14/SMC2 are SMC proteins, while Cnd1, Cnd2/kleisin, and Cnd3 are the three non-SMC proteins that bind to the SMC head domain. (*B*) Genes identified as suppressors for *cnd* mutants form the SUMOylation pathway. (*C*) SUMOylation mutations that suppressed *cnd1*, *cnd2*, and *cnd3* ts mutants. The majority of them are in the SUMO E3 ligase gene pli1. (*D*) Location of suppressor mutations in the 3D structure of SUMO, Hus5/Ubc9, and Pli1 (PDB ID code 5JNE) (*Materials and Methods*). (*E*) Spot tests showed extragenic suppression of *cnd1*, *cnd2*, and *cnd3* mutants by deletion of the pli1 gene, which encodes SUMO E3 ligase. WT, wild type. (*F*) Immunoblotting of WT or Δ*pli1* in the background of the β-tubulin mutant *nda3-KM311* cultured at 33 °C (asynchronous culture) and 20 °C (restrictive temperature, 8 h; cells were arrested at prometaphase) was performed. The upper SUMO bands (red arrows) were detected for Cnd2, Cnd3, and Cut3 in the WT and were abolished in the deletion mutant Δ*pli1*. (*G*) Block and release experiment was done using the ts *cdc25-22* mutant. These cells were blocked in late G2 phase and released synchronously into mitosis by a temperature shift from the restrictive temperature, 36 °C, to the permissive temperature, 26 °C. Aliquots were taken every 15 min for immunoblotting and measurement of the septation index. Cnd2, Cnd3, and Cut3 clearly produced upper bands (red arrows) only during mitosis. Cells of two nuclei without (w/o) septum are mitotic cells, while cells with (w/) septum are postmitotic, but before cytokinesis. The protein bands, that are not SUMOylated, were indicated by black arrows in *F* and *G*.

(9, 18, 19). Together, the hinge segments form a doughnut-shaped structure with two (north and south) interfaces (20). Rad21 associates with the Psm1 head and the Psm3 coiled coil adjacent to the head (21–26). Separase Cut1 is activated when securin Cut2 is ubiquitinated by the anaphase-promoting complex/cyclosome complex and degraded by the 26S proteasome (27, 28), and Cut1 then cleaves residues 179R and 231R of Rad21 (which bridges the head domains of Psm1 and Psm3) during the transition from mitotic metaphase to anaphase (29–31).

In the present study, we intended to examine the interrelationship between condensin and cohesin by isolating many ts cohesin and condensin suppressors in a systematic fashion. If condensin and cohesin share common suppressor genes, the same gene functions might be employed in their complex organization. As the SMC subunits in condensin and cohesin are similar, they may be under similar molecular control. We previously isolated spontaneous suppressors for the ts mutants of the separase/securin protease Cut1–Cut2 complex and found that separase protease is largely dispensable if the interfaces of cohesin subunits become unstable (8). Since the separase protease is specific for cohesin subunit Rad21, we have not yet found any common components that control organization of the cohesin and condensin protein complexes. In this study, we show various distinct suppressors of condensin and cohesin mutants, demonstrating their dissimilar regulation in modifications, recruitment, and protein level. On the other hand, we demonstrate that the N termini of kleisin-like Cnd2 of condensin and Rad21 of cohesin both interact with the hinge directly or indirectly, and this common interaction appears to play a critical role. These interactions may support the "hold and release" model, in which the head and hinge are proximal (8).

Results

Ts/Cold-Sensitive Mutants Selected and Suppressor Screening. Multiple ts/cold-sensitive (cs) mutants in SMC hinge domains or non-SMC subunits (associated with SMC heads) are available for condensin and cohesin, and were selected for suppressor screening in this study. For condensin, ts mutations of three non-SMC subunits

(Cnd1, Cnd2, and Cnd3) were isolated using error-prone mutagenesis (32). *cnd2-1* [containing A114T in the N-terminal helix–turn–helix (HTH) motif] (33) was identified by screening for ts mutants exhibiting chromosome segregation defects. Twelve condensin ts mutants with a single amino acid substitution targeted to the hinge region were also isolated using site-directed mutagenesis (34). For cohesin, *rad21-K1* (containing an effective I67F substitution mutation in the N-terminal HTH motif) (8, 35), *psc3-407* (containing a T234I substitution) (36), and *mis4-242* (containing a G1326E substitution) (37) were identified by screening for ts mutants exhibiting chromosome segregation defects. In addition, six ts and six cs cohesin hinge mutants with a single amino acid substitution were recently isolated (8). A suppressor screening method had been developed and it worked well (7, 8). Therefore, we were able to employ a number of cohesin and condensin mutants to isolate their suppressors.

SUMOylation Impairment Rescues ts *cnd1*, *cnd2*, and *cnd3* Mutants. We obtained suppressors for *cnd1*, *cnd2*, and *cnd3* mutations in condensin non-SMC subunits (Cnd1/NCAPD2, Cnd2/NCAPH, and Cnd3/NCAPG) using previously isolated ts strains: *cnd1-S331P*, *cnd1-H1133P*, *cnd2-A708V*, and *cnd3-K627E* (32). The Cnd subunits associate with the head ATPase domain of condensin SMC subunits Cut3/SMC4 and Cut14/SMC2, as illustrated in Fig. 1*A*. Spontaneous revertants for *cnd1*, *cnd2*, and *cnd3* mutants were isolated, and sites of the extragenic suppressor mutations were determined using whole-genome sequencing. We obtained four classes of suppressor genes, *pmt3*, *rad31*, *hus5*, and *pli1*, which turned out to form the SUMOylation pathway (Fig. 1 *B–D*), consisting of SUMO (Pmt3), SUMO E1-activator (Rad31), SUMO E2-conjugating enzyme (Hus5/Ubc9), and SUMO E3-ligase (Pli1). Suppressor mutation sites obtained, and original ts mutants (used for suppressor screening) are provided (Fig. 1*C*). The great majority of suppressors were obtained from the ligase gene. All four of the genes are essential for SUMOylation (38–41). All substituted amino acids involved are conserved among species (*SI Appendix*, Fig. S1). Thirteen independent suppressors were identified in *pli1* and five of them are single amino acid substitutions. Except for A70E, all of the other four single amino acid substitution events are mapped in Pli1's SP-RING domain (*SI Appendix*, Fig. S1 *D–F*). All nonsense mutations are located N-terminal to the SP-RING domain (*SI Appendix*, Fig. S1*D*). Thus, suppression of the condensin non-SMC mutants' ts phenotype is mostly mediated by inactivation of the SUMOylation pathway.

The ligase deletion mutant Δ*pli1* strongly suppressed the ts phenotype of *cnd1-L685P*, *cnd2-A708V*, and *cnd3-K627E* (Fig. 1*E*). A potentially SUMOylated band could be detected for FLAG-tagged Cnd2 (anti-FLAG antibody), Cnd3 (anti-Cnd3 antibody), and HA-tagged Cut3/SMC4 (anti-HA antibody) proteins only in mitotically arrested cells using *nda3-KM311* (*Materials and Methods* and Fig. 1*F*). No upper band (potential SUMOylation band) could be detected for Cnd1 or Cut14/SMC2, however. Notably, the upper bands (for Cnd2, Cnd3, and Cut3) (Fig. 1*F*) disappeared in Δ*pli1* deletion mutant cells. To confirm that condensin SUMOylation occurs in mitosis, cells containing the *cdc25-22* ts mutation were blocked in late G2 phase and then released synchronously into mitosis by a temperature shift from the restrictive (36 °C) to the permissive (26 °C) temperature. Consistently, the appearance/disappearance of the upper SUMOylated bands coincided with the timing of progression from mitotic metaphase to anaphase (42) (Fig. 1*G*). These results suggested that while condensin SUMO function is apparently concealed in the wild type, ts *cnd* mutant defects were partly restored by deletion of SUMOylation. None of the cohesin non-SMC ts mutants (*psc3-407*, *mis4-G1326E*, and *rad21-K1*) could be rescued by Δ*pli1* (*SI Appendix*, Fig. S2*A*). No cohesin non-SMC protein band showed any change in Δ*pli1* mutant (*SI Appendix*, Fig. S2*B*).

Cnd3 K870 Is the SUMOylation Site, and *cnd3-K870R* Mutant Rescues *cnd2-A708V*. Køhler et al. (43) reported that Cnd3-K824 and Cnd3-K870 may be the sites of SUMOylation (Fig. 2*A*). We constructed two chromosomally integrated substitution mutants containing Cnd3-K870R or Cnd3-K824R, in which Cnd3 could not associate with SUMO. The upper SUMOylation band of Cnd3 was abolished in Δ*pli1* and also in the *cnd3-K870R* chromosomally substituted mutant, but not in *cnd3-K824R*, indicating that K870 may be the actual SUMOylation site (Fig. 2*B*). Suppression of *cnd2-A708V* by *cnd3-K870R* indicated that the failure of C-terminal SUMOylation of Cnd3 in *cnd3-K870R* alleviates the *cnd2-A708V* ts phenotype (Fig. 2*C*). Therefore, loss of Cnd3 K870 SUMOylation partially resembles the effects of loss of SUMOylation on condensin. Cnd3 K870 is conserved among the four fission yeast species (Fig. 2*D*).

Cnd2 May Have a Hooked Structure, and Its N Terminus May Interact with the Cut14 Head-Coiled Coil Junction. Condensin kleisin-like subunit Cnd2 contains an HTH motif at its N terminus and a winged helix domain (WHD) at its C terminus (44) (*SI Appendix*, Fig. S3*A*). Two *cnd2* ts mutants have been previously isolated. One of them contains an A114T substitution in the N-terminal HTH motif (33), and the other contains an A708V substitution in the C-terminal WHD domain (32) (*SI Appendix*, Fig. S3*A*). We were able to isolate three suppressors in *cut14* and two in *cnd2* for *cnd2-A114T* mutant (*SI Appendix*, Fig. S3*B*). In contrast, many more suppressors for *cnd2-A708V* were obtained, as shown in *SI Appendix*, Fig. S3*C*. One of them is extragenic *cut3-S1292I*, which is situated close to the original Cnd2-A708V mutation in the 3D structure (*SI Appendix*, Fig. S3*E*).

All three *cut14* suppressor mutations for *cnd2-A114T* were mapped onto the 3D structure at the head-coiled coil junction, and they are situated close to the original mutation A114T site in the structure (21) (*SI Appendix*, Fig. S3*D*). The results are reminiscent of cohesin's kleisin-like subunit mutant *rad21-K1* (the responsible mutation, I67F, is located in the HTH motif of Rad21), suppressors of which were mapped in the Psm3 head-coiled coil junction (figure 3A of ref. 8). Again, gratifyingly, the

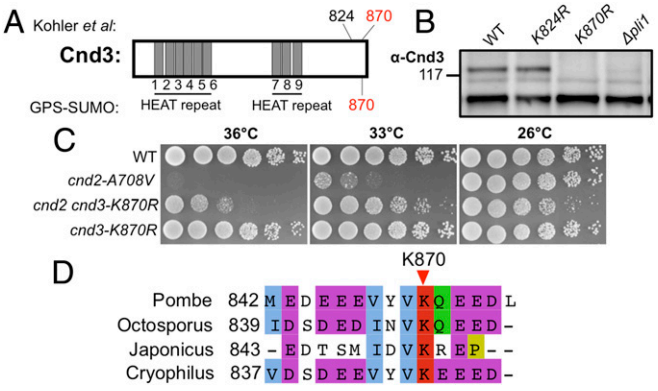

Fig. 2. Cnd3 K870 is the responsible SUMOylation target. (*A*) Potential SUMOylation target sites in Cnd3 identified in a proteome-wide study (43) or predicted by GPS-SUMO software (86). Cnd3 K870 was identified by both methods. (*B*) K870 may be the sole SUMOylation target in Cnd3, as the Cnd3 SUMOylation band (upper band) disappeared in the *cnd3-K870R* mutant. The cs mutant, *nda3-KM311*, was used to arrest cells in mitosis (20 °C, 8 h). (*C*) *cnd3-K870R* rescues the *cnd2-A708V* ts mutant, which resembles those of Δ*pli1* in Fig. 1*E*. (*D*) Conservation of Cnd3 K870 among four fission yeast species: *S. pombe*, Schizosaccharomyces *octosporus*, Schizosaccharomyces *japonicus*, and Schizosaccharomyces *cryophilus*.

cnd2-A708V suppressor mutation, Cut3-S1292I, was mapped to its head, close to Cnd2-A708, according to the structure determined by Bürmann et al. (21) (*SI Appendix*, Fig. S3*E*). These suppressors might restore the protein–protein interaction impaired by the original ts mutations; therefore, suppressor localizations of cnd2 ts mutants indicated that the N terminus of Cnd2 might interact with the Cut14 coiled coil at the head and that the C terminus of Cnd2 might interact with the Cut3 head domain (*SI Appendix*, Fig. S3*F*). In cohesin, the Rad21 N terminus interacts with the Psm3 coiled coil at the head and the Rad21 C terminus interacts with the Psm1 head, so judging from the modes how kleisins bind to SMC heads, Cut14 and Cut3 may be the counterparts of Psm3 and Psm1, respectively.

Except for extragenic suppressor mutations in the SUMOylation pathway, *cnd2-A708V* suppressors were mapped in the Cnd1 C terminus and Cnd2 itself (*SI Appendix*, Fig. S3 *C* and *G*). Four intragenic suppressors of *cnd2-A708V* were mapped to a narrow central region (aa 312–318) far from the original ts mutation site, located at the C terminus (*SI Appendix*, Fig. S3*G*). Therefore, Cnd2 may have a hooked structure (45). Since six suppressors of *cnd2-A708V* were mapped to the Cnd1 C terminus, the Cnd2 C terminus may interact with the Cnd1 C terminus (*SI Appendix*, Fig. S3*G*). A cartoon (*SI Appendix*, Fig. S3*H*) illustrates the possible structural organization of Cnd2 and its interaction with the Cnd1 C terminus.

Proteasome Deficiencies Rescue ts *cnd3-L269P*. Then, using suppressor screening, we found that *cnd3-L269P* was rescued by any of 10 proteasome mutants (*SI Appendix*, Fig. S4*A*). Spot tests for *cnd3-L269P* are shown in *SI Appendix*, Fig. S4*B*, and *cnd3-L269P* was rescued by proteasome deletion mutants Δ*pre9*, Δ*rpt4*, and Δ*rpn10*. Therefore, the rather strong suppression of the ts *cnd3* phenotype resulted from blocking proteasome-mediated proteolysis. Blocking ubiquitin-mediated protein destruction may alleviate the defect of *cnd3-L269P*. In the single *cnd3* mutant, the mutant *cnd3* protein band in SDS/PAGE was less intense than that of wild type (*SI Appendix*, Fig. S4*C*). Band intensity was restored in the double mutant (*cnd3* Δ*pre9*) (*SI Appendix*, Fig. S4*C*) at both the permissive and restrictive temperatures, suggesting that suppression was due to an increase of *cnd3* mutant protein, which failed to be destroyed in proteasome mutants. We provided evidence that Cnd3 mutant protein is unstable and that this instability was restored in proteasome mutants in the presence of the protein synthesis inhibitor cycloheximide (46) (*SI Appendix*, Fig. S4*D*).

Rescue of *rad21* and *psc3* Mutants by the Loss of RNA Elimination Factors. Suppressor screening and subsequent analysis of identified suppressors were conducted for the cohesin ts mutants *rad21-K1, psc3-T234I* (T234I is the responsible mutation of *psc3-407*), and *psc3-S931Stop* (S931Stop is the responsible mutation of *psc3-303*) (35, 36). We obtained 20 suppressors belonging to a group of mRNA catabolic (elimination) factors: *erh1*/*new10*, *mmi1*, and *red1* (47–49) (Fig. 3*A*). For example, spot test results show suppression of the *psc3* and *rad21* mutants by Δ*red1* (Fig. 3*B*). Eight suppressors of *rad21-K1* reside in the *erh1*/*new10* gene (Fig. 3*A*). ERH is a small, highly conserved, but enigmatic protein implicated in heterochromatin domain assembly (50, 51). It seems to play an important role in the cell cycle through its transcript-splicing activity and is critically required for genomic stability and cancer cell survival (52). Two *mmi1* suppressors in the RNA-binding YTH domain (47, 53) are shown in Fig. 3*C*, and the mutations may directly disrupt its ability to bind RNA. Thus, the loss of RNA elimination restores the mitotic sister chromatid cohesion in *rad21* and *psc3* mutants. However, how cohesion-defective mutations are rescued by the loss of RNA elimination is not well understood.

Cohesin Mutant *mis4-G1326E* was Rescued by the Loss of Chromatin Remodeling Factor Hrp1. Suppressor screening was extended to a cohesin loading factor ts mutant, *mis4-G1326E* (37), and a number of suppressors were obtained and found to be derived from the *hrp1* locus (Fig. 3*D*). The genetic interaction between the Mis4/NIPBL defective in cohesin loader and chromatin remodeling factor Hrp1 is highly selective, and of considerable interest. Mutations indicated in blue in Fig. 3*D* are nonsense mutations that introduced premature stop codons into the *hrp1* gene, while those in green are substitutions, which were broadly distributed in the chromodomain, SNF2-like domain, helicase domain, and homeodomain. Suppression seems to be evoked by any one of many mutations. Hrp1 single amino acid substitutions are shown in a nucleosome–Hrp1 complex structure (54) (Fig. 3*E*). The deletion mutant Δ*hrp1* (but not Δ*hrp3*) rescued *mis4-G1326E* too (Fig. 3*F*). Mis4 and Hrp1 were copurified with a heterochromatic protein, Swi6/HP1 (55, 56); therefore, Hrp1 may mediate the connection of cohesin with chromosomal nucleosome and heterochromatic proteins such as Swi6/HP1. In addition, Mis4 human homolog NIPBL is the causal gene of Cornelia de Lange syndrome (57, 58), and the suppression of *mis4* by *hrp1* mutations may offer clues to treat the disease.

Suppression of Condensin Hinge Mutants by Kleisin-Like *cnd2* and SMC Head Mutations. For screening suppressors of condensin hinge mutants, we employed nine of the 11 condensin hinge ts mutants (34). Only two strains, *cut3-G777E* and *cut14-G655E* (locations of the substitutions in a hinge structure are shown in Fig. 4*C*), yielded four suppressors in the non-SMC Cnd2 gene that rescued the ts phenotype of the hinge mutant *cut3-G777E* or *cut14-G655E* (Fig. 4 *A* and *B*). In addition, one SMC *cut3* mutation, M1218R, rescued the hinge *cut14-G655E* mutation (Fig. 4*A*). Note that Cut14 G655 and Cut3 G777 are located at the same positions in the amino acid alignment, but in the 3D structure, they reside at different interfaces of the hinge. In the 3D hinge structure, locations of these two residues are symmetrical under 180° rotation, as the heterodimeric hinge has approximately twofold rotational symmetry (Fig. 4 *C* and *G*). Curiously, the hinge suppressor in Cut3/SMC4 (M1218R) resided in the head domain, while the other four were located in the N terminus of kleisin-like Cnd2 (T117I, G142R, G142E, and A144V) (Fig. 4*A*).

We looked at Cnd2 substitutions, and found that Cnd2-T117, Cnd2-G142, and Cnd2-A144 are all located in the same helix of the conserved HTH motif at its N terminus (Fig. 4*H* and *SI Appendix*, Fig. S5*A*). Note that the *cut3* and *cnd2* suppressors contained bulkier side-chain residues (*SI Appendix*, Fig. S5*B*). Three of the *cnd2* suppressors were only two residues apart (G142E/R and A144V). Two distinct mutations containing larger side-chain residues (E and R) at G142 suppressed the *cut3-G777E* and *cut14-G655E* mutations (discussed below). A simple hypothesis to explain this suppression is that destabilization of the hinge by Cut3-G777E or Cut14-G655E appeared to be compensated for by the second destabilizing mutation (e.g., G142E) in the amino terminus of kleisin-like subunit Cnd2. The hinge and Cnd2 N terminus may directly associate or indirectly interact through, for example, the mediation of DNA (*Discussion*).

Cohesin Hinge Mutants Are Rescued by Kleisin-Like *rad21* and STAG-Like *psc3* Mutations. Similar suppressor screening was conducted for cohesin hinge mutants isolated previously (8). Only two cs mutants (*psm3-G653E* and *psm1-G661E*) yielded three distinct spontaneous suppressors in non-SMC cohesin subunits, Rad21 and Stag-like Psc3 (Fig. 4 *D* and *E*). Psm3-G653E and Psm1-G661E are located at different hinge interfaces (Fig. 4*F*) and are conserved in condensin Cut3/SMC4 and Cut14/SMC2 subunits too (Fig. 4*G*). All condensin and cohesin hinge

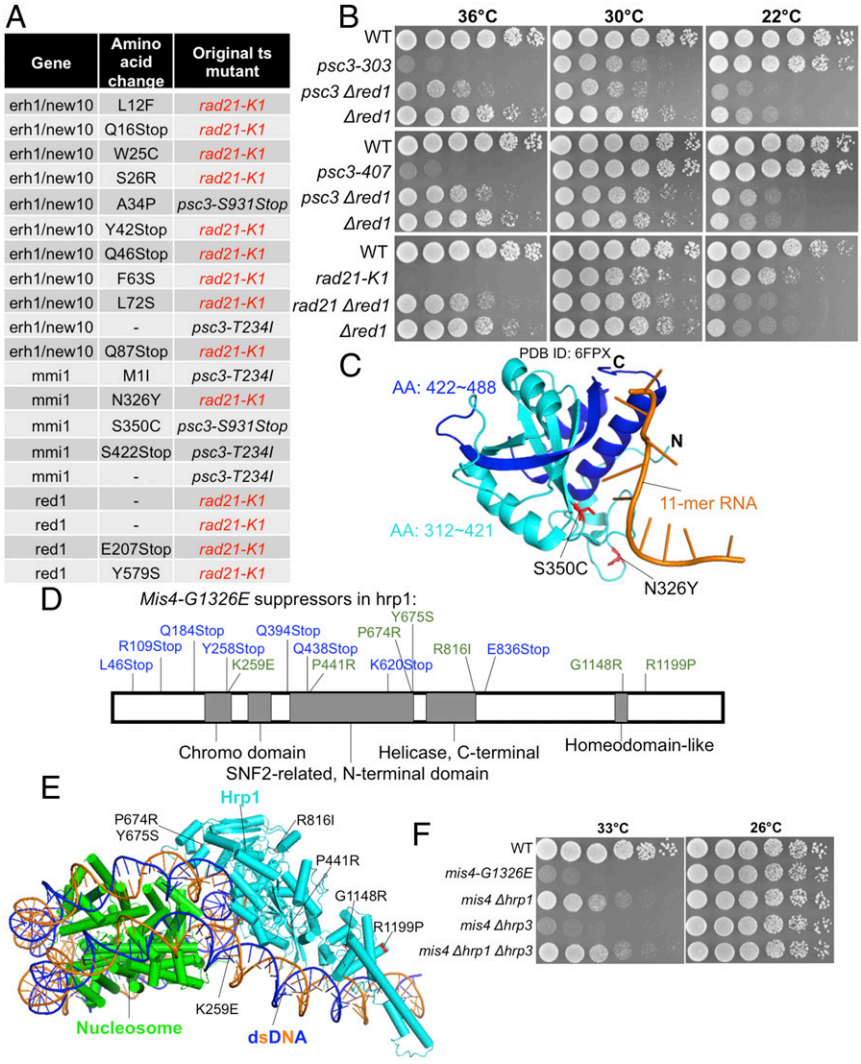

Gene	Amino acid change	Original ts mutant
erh1/new10	L12F	*rad21-K1*
erh1/new10	Q16Stop	*rad21-K1*
erh1/new10	W25C	*rad21-K1*
erh1/new10	S26R	*rad21-K1*
erh1/new10	A34P	*psc3-S931Stop*
erh1/new10	Y42Stop	*rad21-K1*
erh1/new10	Q46Stop	*rad21-K1*
erh1/new10	F63S	*rad21-K1*
erh1/new10	L72S	*rad21-K1*
erh1/new10	-	*psc3-T234I*
erh1/new10	Q87Stop	*rad21-K1*
mmi1	M1I	*psc3-T234I*
mmi1	N326Y	*rad21-K1*
mmi1	S350C	*psc3-S931Stop*
mmi1	S422Stop	*psc3-T234I*
mmi1	-	*psc3-T234I*
red1	-	*rad21-K1*
red1	-	*rad21-K1*
red1	E207Stop	*rad21-K1*
red1	Y579S	*rad21-K1*

Fig. 3. Suppressors of *rad21-K1*, *psc3-T234I*, and *psc3-S931Stop* reside in *erh1/new10*, *mmi1*, and *red1* loci, all of which are involved in mRNA elimination. (*A*) Suppressors in e*rh1/new10*, *mmi1*, and *red1* that were obtained as spontaneous suppressors for ts *rad21* and *psc3*. (*B*) Suppression of the ts phenotype of *psc3* and *rad21* by Δ*red1* is shown. The Δ*red1* is cs. WT, wild type. (*C*) Mmi1 mutations in an Mmi1 structure in complex with an 11-mer RNA (PDB ID code 6FPX) (*Materials and Methods*). Mmi1 contains a YTH domain at its C terminus that binds specific RNA sequences. Mmi1-S326 and Mmi1-S350 were located in Mmi1's YTH domain. Mmi1-S326Y and Mmi1-S350C mutations may disrupt Mmi1's ability to bind RNA directly. Mmi1-S422Stop causes loss of the Mmi1 C terminus (blue); therefore, it cannot bind RNA. AA, amino acid. (*D*) *mis4-G1326E* extragenic suppressors were mapped onto a chromosome remodeling factor gene, hrp1. (*E*) Hrp1 mutation in a nucleosome-Hrp1 structure (PDB ID code 5O9G) (*Materials and Methods*). (*F*) Δ*hrp1* (but not another chromosome remodeling factor mutant, Δ*hrp3*) rescued *mis4-G1326E* at 33 °C too.

mutations that were rescued by mutations in the SMC head or non-SMC subunits are substitutions of G residues (to E residues) in the conserved GX6GX3GG sequence motif, which is normally found in hinge dimerization interfaces. Both the Rad21-W23S and Rad21-M84K suppressors reside in the N-terminal domain (Fig. 4*H* and *SI Appendix*, Fig. S5*C*). The cs phenotypes of *psm3-G653E* and *psm1-G661E* were rescued by these suppressing mutations (Fig. 4*E*). Psc3 contains multiple HEAT repeats, and the mutation Psc3-D388N resides in the repeat (59). This mutation may affect the affinity of Psc3 for DNA binding (*SI Appendix*, Fig. S5*D*). It is clear that the two hinge residues Psm1-G661 and Psm3-G653, located at the hinge interfaces (Fig. 4*F*), and bulkier side-chain amino acids (from G to E), causing destabilization of the interfaces, were introduced. Suppressor residues showed the change from W→S and from M→K, significantly altered in their side-chain properties (from aromatic to hydrophilic and from hydrophobic to basic) (*SI Appendix*, Fig. S5*E*). It remains to be determined whether these changes restored the physically destabilized hinge.

Condensin and Cohesin Hinge Suppressors Reside in the N-Terminal Domain of Rad21 and Cnd2. Cnd2 and Rad21 proteins are kleisin-like homologous subunits of condensin and cohesin, respectively. As suppressors of the hinge located in the N termini of Cnd2 and Rad21, we prepared the alignment of suppressor mutation sites. Rad21-W23S, Rad21-M84K, cnd2-T117I, cnd2-G142E/R, and cnd2-A144V are all arranged in the same N-terminal domain (Fig. 4*H*). Strikingly, Rad21-M84K and Cnd2-G142E/R differed at only one residue, strongly suggesting that the rescue of hinge defects by the suppressors in kleisin-like subunits might occur through highly similar mechanisms in condensin and cohesin, consistent with the hypothesis that hinge structure and function are coupled with the HTH structure (or helix bundle; Fig. 4*I*) formed by the N terminus of kleisin-like Cnd2 and Rad21. Implications of these findings are discussed below (*Discussion*).

Rescue of Cohesin Hinge Defects by *wpl1* or *pds5* Mutations. We found that cohesin cs hinge mutants were also rescued by mutations in Wpl1 and Pds5, which associate with the cohesin head and act as cohesin-releasing factors (60–62). This suppression occurs in both *psm1* and *psm3* hinge cs mutants. Single amino acid substitutions in the *wpl1* gene that suppressed *psm1* or *psm3* cs mutants are shown in Fig. 5*A*. Two *pds5* mutants could also suppress *psm1* and *psm3* hinge mutations, while ∼60 *wpl1* suppressors were obtained for *psm1* and *psm3* hinge mutants. Since Wpl1 forms the complex with Pds5, this result suggested that the *wpl1* mutant is the main extragenic suppressor gene for the *psm1* and *psm3* hinge. We mapped Wpl1 mutations onto the structure (Fig. 5*B*) and found that they are all located on the surface (62, 63). These mutations may disrupt the physical interaction between Wpl1 and Rad21 and further Wpl1's association with Rad21. Fig. 5*C* and *SI Appendix*, Fig. S6*A* show spot tests of

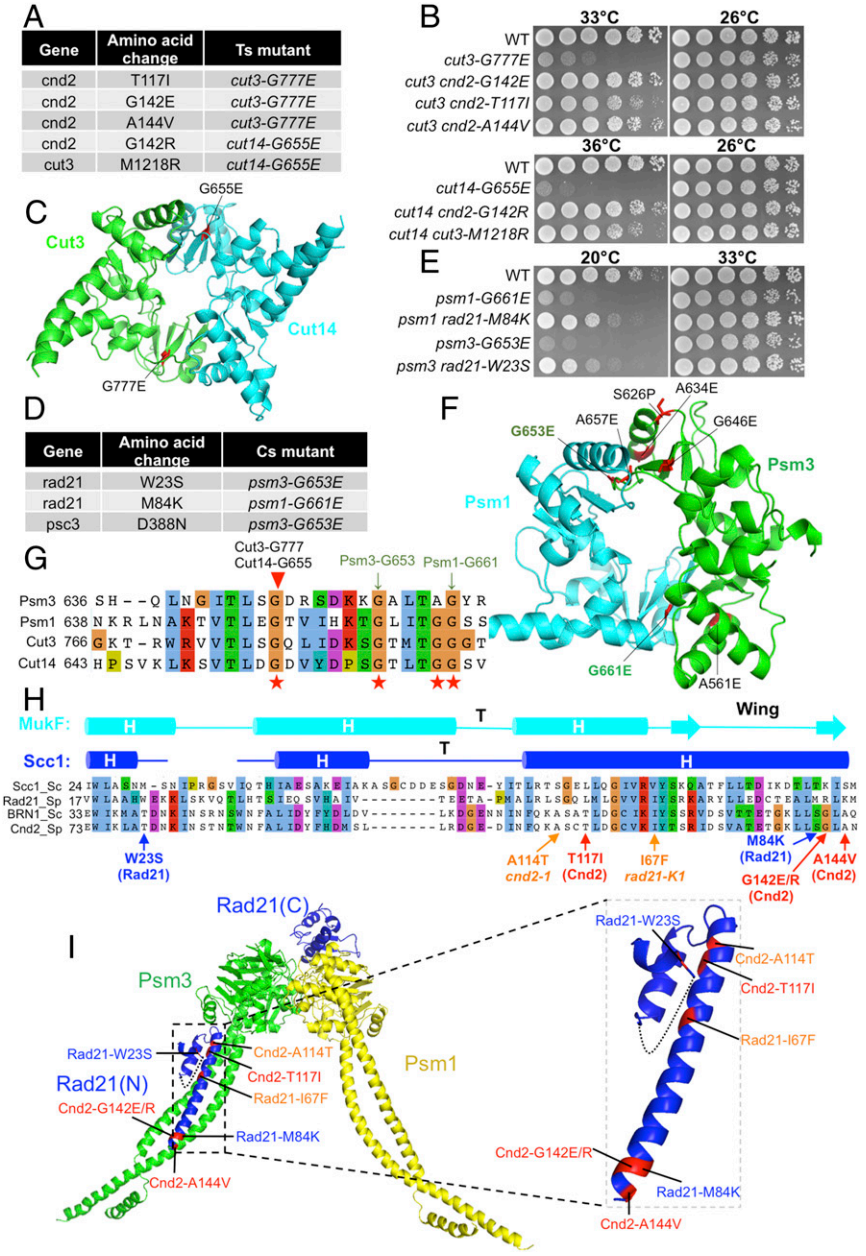

Fig. 4. Suppressors of condensin hinge ts mutants and cohesin hinge cs mutants. (*A*) Suppressors in the cnd2 and cut3 head domain obtained from condensin hinge ts mutants (*cut3-G777E* and *cut14-G655E*). (*B*) Suppression of the condensin hinge ts mutants by the suppressors in *A*. WT, wild type. (*C*) Localization of Cut14-G655E and Cut3-G777E in the condensin hinge structure. Both mutations are located in hinge dimer interfaces. (*D*) Suppressors in *rad21* and *psc3* obtained from cohesin hinge cs mutants. (*E*) Suppression of cohesin hinge cs mutants by the suppressors in *D*. (*F*) Localization of Psm3-G653E and Psm1-G661E in the cohesin hinge structure. (*G*) Localization of the corresponding condensin hinge ts mutations in *A* and cohesin hinge cs mutations in *D* in a protein alignment of the hinges. (*H*) Localization of condensin hinge and cohesin hinge suppressors in a protein alignment of kleisin N termini. The secondary structure is predicted based on the structure of the *S. cerevisiae* Scc1 N terminus. Condensin hinge suppressors are shown in red, and cohesin hinge suppressors are shown in blue. In addition, responsible mutations of ts mutants *cnd2-1* (A114T) and *rad21-K1* (I67F) that are located in their N termini are shown (orange). (*I*) Localization of the mutations from *H* in the structure. All of them may directly affect kleisin's interaction with the SMC head-coiled coil junction. Condensin hinge suppressors (Cnd2-T117I, Cnd2-G142E/R, and Cnd2-A144V) and cohesin hinge suppressors (Rad21-W23S and Rad21-M84K) may enhance kleisin's interaction with the SMC head-coiled coil junction, while the *cnd2-1* mutation A114T and *rad21-K1* mutation I67F may disrupt this interaction.

cohesin hinge cs mutants' suppression by Δ*wpl1*, while cohesin hinge ts mutants cannot be rescued (*SI Appendix*, Fig. S6*B*).

Rad21/Scc1 is hyperphosphorylated (17, 64), and it may serve as an indicator of functional cohesin (8). Immunoblotting using an anti-Rad21 polyclonal antibody indicates that Rad21 phosphorylation decreased greatly in cohesin hinge cs mutants (Fig. 5*D*); not only Rad21 phosphorylation but the Rad21 protein level also decreased greatly in cohesin hinge ts mutants (*SI Appendix*, Fig. S7*A*). Therefore, cohesin hinge cs mutants may disrupt sister chromatid cohesion. Cohesin hinge ts mutants may not only disrupt sister chromatid cohesion but also cause a decrease of cohesin protein levels. Actually, Rad21 is fully phosphorylated in Δ*wpl1*, and the Rad21 phosphorylation level in cohesin hinge cs mutants is rescued by Δ*wpl1*, while the loss of the Rad21 protein level in cohesin hinge ts mutants cannot be rescued by Δ*wpl1* (Fig. 5*E* and *SI Appendix*, Fig. S7*B*). These results explain Cut1/separase ts mutants' suppression by these cohesin hinge mutants, as observed in the study by Xu et al. (8): Either loss of cohesion (in cohesin hinge cs mutants) or reduction of cohesin abundance (in cohesin hinge ts mutants) rescued defective cleavage of cohesin (and its release from chromatin) in Cut1/separase ts mutants.

Suppression of Condensin Hinge Mutants by Loss of Kinases and a Phosphatase. Two condensin hinge ts mutants (*cut14-L608P* and *cut14-G655E*) were rescued by multiple mutations in kinase genes (*sck1*, *sck2*, and *ksg1*) and Ppe1/PP6 phosphatase complex genes (*ppe1* and *ekc1*) (65) (*SI Appendix*, Fig. S8*A*). Ppe1 is similar to human PP6. Spot test results are shown in *SI Appendix*, Fig. S8*B*. Chromosome segregation defects of *cut14-L608P* were partially rescued by a phosphatase deletion mutant Δ*ppe1*: Sister chromatids were segregated but unequal, as large and small daughter nuclei were observed frequently (*SI Appendix*, Fig. S8*C*), suggesting that centromeric function was impaired in the double mutants, which is consistent with the Ppe1–Ekc1 phosphatase complex's role in the centromere/kinetochore (66).

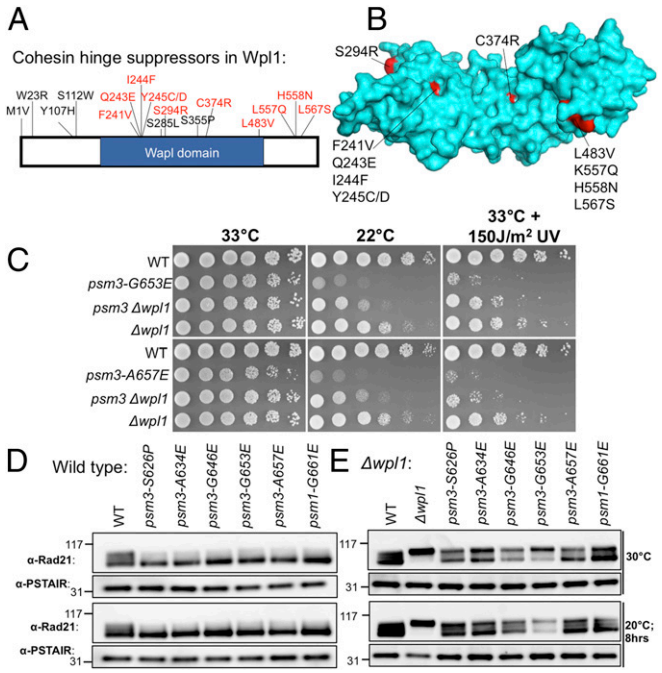

Fig. 5. Suppression of cohesin hinge cs mutants by *wpl1*. (*A*) Localization of single amino acid substitutions in Wpl1 protein that rescued cohesin hinge cs mutants. Fifty-nine suppressors in wpl1 that suppressed cohesin hinge cs mutants were obtained, and some of them are nonsense mutations or indels. (*B*) Localization of the mutation sites on the Wpl1 structure (PDB ID code 3ZIK) (*Materials and Methods*). (*C*) Suppression of cohesin hinge cs mutants by Δ*wpl1* (more spot results are shown in *SI Appendix*, Fig. S6*A*). These cohesin hinge cs mutants are hypersensitive to UV light. The UV sensitivity of these cs mutants was rescued by Δ*wpl1* too (more spot results are shown in *SI Appendix*, Fig. S6*A*). WT, wild type. (*D*) Rad21 phosphorylation level in WT and cohesin hinge cs mutants detected using an anti-Rad21 polyclonal antibody (17, 64). Rad21 phosphorylation serves as an indicator of functional cohesin (8). (*E*) Rad21 phosphorylation level in WT, Δ*wpl1*, and *hinge* Δ*wpl1* double mutants. Wpl1 and Pds5 bind the cohesin head and function as cohesin-releasing factors.

Mutation localization mapping onto the protein sequence indicated that mutations were enriched in kinase domains of Sck1 and Ksg1 (*SI Appendix*, Fig. S8*D*); therefore, loss of their kinase activities rescued condensin hinge ts mutants. Sck1 mutations were located in the cleft that binds a nonhydrolyzable ATP analog 5′-adenylyl-imidodiphosphate (AMP-PNP) directly (67) (*SI Appendix*, Fig. S8*E*), while Ksg1 mutations might not affect ATP binding directly (68) (*SI Appendix*, Fig. S8*F*). Ksg1 is an essential gene and similar to human PDPK. Whether these kinases and phosphatase directly affect condensin hinge phosphorylation remains to be clarified.

Discussion

In this study, we employed many *ts* or *cs* cohesin and condensin mutants of SMC hinge domains and also head-associated non-SMC subunits, and obtained numerous spontaneous suppressors, genomic loci of which were determined by whole-genome sequencing. Presumed gene functions of suppressors suggested that distinct pathways are implicated in the rescue of *ts* or *cs* phenotypes of condensin and cohesin mutants. In condensin, SUMOylation pathway mutants and 26S proteasome protein destruction mutants suppressed mutants of head-interacting non-SMC subunits. Protein phosphorylation/dephosphorylation was involved in rescuing condensin hinge mutants, because mutations in protein kinases (Ksg1, Sck1, and Sck2) and a phosphatase complex (Ppe1 and its regulatory subunit Ekc1) were identified (Fig. 6*A* and *SI Appendix*, Fig. S8). ATPase-dependent auto-phosphorylation of the condensin hinge was previously shown to diminish the DNA-binding ability of the hinge (69), suggesting that hinge phosphorylation resulted in the decline of the DNA-binding ability of condensin. If Ppe1 phosphatase acts on the hinge and hinge phosphorylation were up-regulated by kinases, the loss of Ppe1 might enhance hinge phosphorylation.

In cohesin, on the other hand, mutants of RNA elimination pathways (*new10*, *red1*, and *mmi1*) or *hrp1* mutant defective in chromatin remodeling suppressed the mutants of three head-interacting cohesin non-SMC subunits (*rad21*, *psc3*, and *mis4*). In addition, cohesin hinge *cs* mutants were rescued by mutations in cohesin-releasing factors (*wpl1* and *pds5*) (Fig. 6*B*). Hence, although condensin and cohesin are similar in that both complexes contain SMC and non-SMC kleisin subunits, they are regulated by distinct pathways. We have not yet found suppressors of cohesin implicated in SUMOylation, ubiquitination, or phosphorylation/dephosphorylation. Judging from the putative

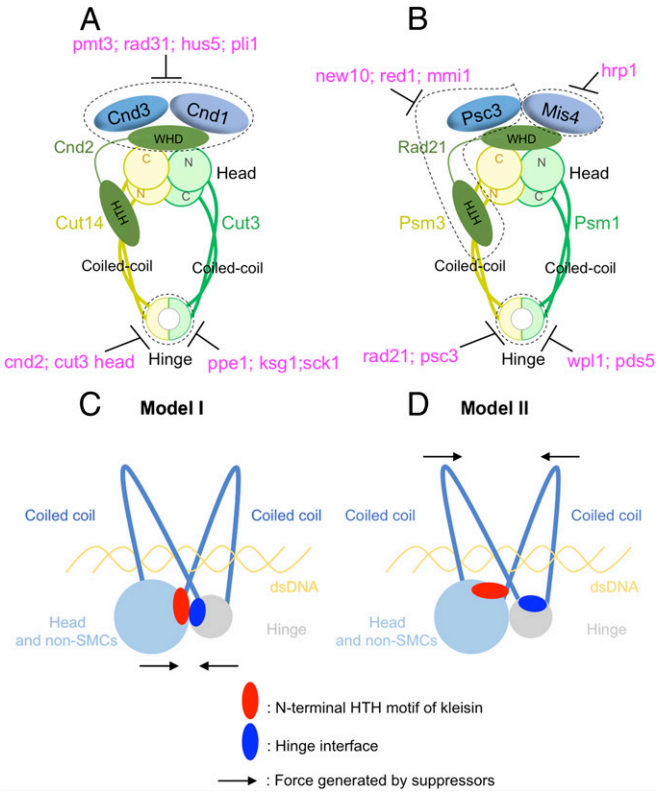

Fig. 6. Condensin and cohesin are regulated differently, but they may adopt a similar organization in which the hinge and head interact. (*A*) Summary of condensin's suppression by SUMOylation pathway mutants (*pmt3*, *rad31*, *hus5*, and *pli1*), kinase or phosphatase mutants (*ppe1*, *ksg1*, and *sck1*), and condensin mutants (*cnd2* and *cut3* head mutations). (*B*) Summary of cohesin's suppression by RNA elimination pathway mutants (*new10*, *red1*, and *mmi1*), chromatin-remodeling factor mutants (*hrp1*), cohesin-releasing factor mutants (*wpl1* and *pds5*), and cohesin non-SMC mutants (*rad21* and *psc3*) (text). Two models were proposed in *C* and *D* to explain SMC hinge interface mutants' suppression by mutations in the N-terminal HTH motif of kleisins. (*C*) SMC hinge interfaces and the N-terminal HTH motif of kleisins may interact directly to form arched coiled coils, which hold and release chromosomal DNA. SMC hinge interface mutations may impair head–hinge interaction, and suppressors in the N-terminal HTH motif of kleisins rescue the interaction. (*D*) SMC hinge interfaces and the N-terminal HTH motif of kleisins may not directly interact, but they both regulate coiled-coil orientation. SMC hinge interface mutations may widen the coiled-coil angle, thereby impairing the capacity of the coiled coils to hold chromosomal DNA. Suppressors in the N-terminal HTH motif of kleisins rescue the DNA-binding ability of the coiled coils.

roles of cohesin suppressors, cohesin may be regulated by protein [and possibly RNA (70)] loading/releasing rather than modification-reverse modification, as seen in condensin.

We showed that three condensin subunits (Cnd2, Cnd3, and Cut3) are SUMOylated during mitosis, and our results suggest that SUMOylation antagonizes the function of non-SMC subunits. K870 is the candidate SUMOylation site in Cnd3, as K870R mutation abolishes the band of putative SUMO-bound Cnd3. The rescue of *cnd2-A708V* by *cnd3-K870R* indicates that the K870R mutant resembles the SUMOylation loss phenotype. Therefore, SUMOylation at Cnd3 K870 may weaken non-SMC subunits' function; thus, temperature sensitivity was rescued in *cnd* Δ*SUMO* double-mutant cells. To examine the effects of SUMOylation loss on condensin, we observed phenotypes of the *cnd3-K627E* single mutant and *cnd3-K627E* Δ*pli1* double mutant at permissive (26 °C) and restrictive (36 °C) temperatures (*SI Appendix*, Fig. S9*A*). The *cnd3-K627E* exhibited typical segregation defects observed in condensin mutants. This defect was rescued in the *cnd3-K627E* Δ*pli1* double mutant, but large and small daughter nuclei, which are typical phenotypes of centromere mutants, were newly observed (*SI Appendix*, Fig. S9*A*). Therefore, loss of SUMOylation partially rescued condensin ts mutants' segregation defects but, at the same time, caused a unique centromeric segregation defect, suggesting that SUMOylation might protect centromeric function in mitosis. Consistently, mitotic condensin is bound to active genes as well as to central centromeric chromatin (71–73), and condensin non-SMC subunits may have a kinetochore/centromere function (32). Actually, although the temperature sensitivity of *cnd3-K627E* was rescued by Δ*pli1*, double mutants' sensitivity to thiabendazole (TBZ, a microtubule destabilizing drug) was additive (*SI Appendix*, Fig. S9*B*). These results suggested that SUMOylation may act distinctively at chromosome arms and centromeres during mitosis. In addition to cohesin and condensin, there is one more SMC complex, the Smc5–Smc6 complex, and it affects kinetochore protein SUMOylation (74). Therefore further experiments are needed to test if the Smc5–Smc6 complex is affected by Δ*pli1* and to clarify whether the centromeric defects observed in *cnd3-K627E* Δ*pli1* were due to loss of condensin SUMOylation.

For condensin and cohesin hinge mutants, suppressors were obtained in kleisin-like Cnd2 and Rad21, respectively (Fig. 4 *A* and *D*). This would indicate that fission yeast kleisin homologs play a common hinge-interacting role in the organization of cohesin and condensin complexes (75). Cnd2 and Rad21 are bound to the SMC heads. Hence, the interaction resulting in suppression may occur between the head and hinge. This presumed head–hinge interaction is consistent with a model of arched coiled coils for DNA binding/dissociation proposed for cohesin (8). The present suppressor screening further revealed the importance of the HTH motif in the N terminus of kleisin, which appears to mediate kleisin homolog's interaction with the SMC (Cut14 in condensin and Psm3 in cohesin) head-coiled coil junction (Fig. 4*I*). This HTH domain may be required for interaction with the hinge and/or DNA.

Surprisingly, condensin ts mutations (*cut3-G777E* and *cut14-G655E*) actually resided at the same positions in the alignment of heterodimeric (Cut3/SMC4 and Cut14/SMC2) hinge sequences (Fig. 4*G*). These mutations, located in β-structures at the central hinge interfaces, presumably destabilize the interfaces, as substitutions were from G to much larger E residues. Four *cnd2* (and one *cut3* head mutation) suppressors were obtained for these two hinge mutants, all located in the amino-terminal HTH-containing helix bundle of Cnd2 (Fig. 4*I*). Three mutations (Cnd2-G142E, Cnd2-G142R, and Cnd2-A144V) resided very closely and were located in the same α-helix (Fig. 4*I*, *Right*). These results strongly suggested the presence of a tightly coupled mechanism to restore hinge mutations by second mutations in the helix bundle of N-terminal Cnd2. To understand the restoration mechanism, further investigation is required. Direct interaction between the hinge and Cnd2 may exist, or, alternatively, indirect interaction mediated by DNA, which may be sandwiched between the arched coiled coils, may exist.

For cohesin, the hinge mutants cs *psm3-G653E* and *psm1-G661E* produced two suppressors, *rad21-W23S* and *rad21-M84K*, located at the HTH in the N terminus, as in the case of *cnd2* suppressors. Strikingly, all four hinge mutants (*cut3-G777E*, *cut14-G655E*, *psm3-G653E*, and *psm1-G661E*) have the same substitutions from G to E located in the same GX6GX3GG sequence motif at the conserved G residues (Fig. 4*G*). This G-rich motif, conserved even in homodimeric prokaryote SMC, is required for hinge dimerization (76–78). We speculate that the helix bundle of the kleisin, which interacts with the SMC head-linked coiled coil, may be important in regulating the coiled-coil orientation. These mutations may restore the capacity of DNA binding, which is defective in hinge mutants, so that the orientation of arched coiled coils might alter the properties of its association/dissociation cycle with chromosomal DNA.

Evidence that interactions between the HTH motif in the helix bundle and the hinge are critical for the role of cohesin and condensin is provided below. Mutations of *rad21-I67F* (8) and *cnd2-A114T* (33) reside in the same HTH of kleisin homologs (Fig. 4 *H* and *I*). These two mutations not only exhibited severe defects in mitotic chromosome segregation but were also highly sensitive to DNA-damaging agents at the permissive temperature. The great majority of SMC hinge suppressors resided in kleisin's HTH motif. Furthermore, hinge interface mutants residing at similar positions generated such HTH suppressor mutations. The actual mechanism of suppression remains to be clarified, while understanding the modes of association and dissociation of DNA with cohesin and condensin is imperatively needed.

In the hold and release model, the hinge interfaces are probably important in regulating coiled-coil orientation, and these G-to-E mutations may weaken the coiled coils' ability to associate with DNA, possibly by widening the angle of the arched coils. Notably, second mutations that suppressed hinge mutations were found in the amino terminal region of kleisin-like Cnd2 and Rad21. Surprisingly, among six suppressors, four of them (*cnd2-A144V*, *cnd2-G142E, Cnd2-G142R*, and *rad21-M84K*) reside closely at the end of the second helix of the HTH motif, close to the ATPase head domain in the 3D structure (Fig. 4 *H* and *I*). The remaining two suppressors, Cnd2-T117I and Rad21-W23S, also reside very closely. One possible explanation for this finding is that the kleisin HTH motif may be critical to the capacity for DNA binding.

In addition to the hold and release model, Skibbens (79) proposed a C-clamp conformation of cohesin, in which SMC coiled coils can fold over into a "C" shape to promote head–hinge association and DNA is entrapped into the C-clamp. Rad50 binds to dsDNA, and its structure (80–82) resembles the SMC Psm1-Psm3 head-coiled coil region (8). From the model of DNA interaction with Rad50 (80–82), in which two coiled coils and a head hold DNA inside, one may speculate that DNA binds to the basic residues on the inner sides of the cohesin coiled coils and head as proposed in the hold and release model (8). We consider two models to explain the mechanism by which hinge mutants were rescued by mutations in the N-terminal HTH motif of kleisins (Fig. 6 *C* and *D*). In the first model, to form arched coiled coils that bind DNA, as in the case of Rad50, the head and hinge need to interact. However, how the head of the holocomplex interacts with the hinge is unclear yet. Head–hinge interaction may require the kleisin N-terminal HTH motif and hinge interfaces, judging from the locations of original mutations and their suppressors in the 3D structure (8, 20–26). Hinge interface mutations may destabilize head–hinge interaction, and suppressor mutations in the kleisin N-terminal HTH motif may

restore the interaction. This restoration occurs by direct interaction between the hinge interface and the N-terminal HTH motif of kleisin that binds to the SMC head region (model I, Fig. 6*C*). In the second model, the N-terminal HTH motif of kleisin subunits and hinge interfaces may not be involved directly in head–hinge interaction, but may instead regulate the orientation of coiled coils that enables them to hold and release DNA. Both coiled coils emerging from head and hinge are required to hold DNA, and they work collaboratively in regulating DNA binding. Hinge interface mutations may weaken the DNA-binding activity of coiled coils at the hinge, but suppressor mutations in the kleisin N-terminal HTH motif may enhance the DNA-binding activity of coiled coils at the head by changing the angle made by arched coiled coils (Fig. 6*D*), therefore balancing DNA binding by the coiled coils.

Materials and Methods

Strains, Plasmids, and Media. Parental *S. pombe* ts strains of cnd1, cnd2, cnd3, rad21, mis4, and the 12 cohesin hinge mutants (six cs and six ts) used for suppressor screens have been described previously (8, 32). Briefly, the responsible ts mutations were reintegrated into the *S. pombe* haploid wild-type strain 972 h^- by site-directed PCR-based mutagenesis to obtain ts mutants with a wild-type background (7). The *cnd3-K824R* and *cnd3-K870R* were constructed using the same method as described above. The Δ*pli1*, Δ*red1*, Δ*erh1*, Δ*hrp1*, and Δ*hrp3* were constructed in a similar way: ∼500-bp sequences before and after the corresponding ORFs were cloned and ligated into pBluescript plasmids with the hygromycin antibiotic resistance gene (hygR) in between; plasmids were linearized and were chromosomally integrated into corresponding endogenous loci of the wild-type strain 972 h^-. Hygromycin-resistant colonies were then picked, and deletion of the responsible genes was verified by PCR. Proteasome complex mutants (Δ*pre9,* Δ*rpn10*, and Δ*rpt4*) and Δ*wpl1*, which contain the KanMX4 selection marker and are resistant to G418, were obtained from an *S. pombe* haploid deletion mutant library (Bioneer Corporation). Parental *S. pombe* strains used for immunoblotting of Cnd1-3FLAG, Cnd2-3FLAG, Cut3-3HA6His, Cut14-3FLAG, Rad21-3FLAG, Psc3-3FLAG, and Mis4-3FLAG have also been described previously (15, 17, 33, 64, 71). YPD (1% yeast extract, 2% polypeptone, 2% D-glucose) and Edinburgh minimal medium 2 were used to culture *S. pombe* strains, and malt extract agar medium was used for sporulation (83).

Suppressor Screening, Next-Generation Sequencing, and Suppressor Identification. An efficient suppressor screening method, which applied genomic DNA mixtures for next-generation sequencing to identify suppressor mutations, was developed (7). Suppressor screening, next-generation sequencing of suppressor genomic DNA mixtures, and suppressor mutation identification followed the same procedure described in that paper by Xu et al. (7).

Synchronous Culture and Temperature Shift Experiments. To arrest cells in mitosis, *nda3-KM311* (a cs β-tubulin mutant)–containing strains were used. The *nda3-KM311* cells fail in mitotic spindle assembly and arrest in prometaphase due to spindle checkpoint activation (84). Cells were first cultured at a permissive temperature of 30 °C (to 4–5 × 10^6 cells per milliliter), and were then shifted to a restrictive temperature (20 °C) for 8 h. For the block and release experiment with the *cdc25-22* mutant (85), cells were grown in YPD at 26 °C (to 3 × 10^6 cells per milliliter, 100 mL) and then shifted to 36 °C for 4 h to block cells in late G2 phase. Cells were then released to 26 °C. The time point of release was treated as the start point (0 min). Then, aliquots (10 mL) were taken every 15 min for immunoblotting and measurement of the septation index.

Fluorescence Microscopy. Cells were cultured to 4–5 × 10^6 cells per milliliter, fixed with 2% glutaraldehyde, stained with DAPI (a fluorescent probe for DNA), and observed under an all-in-one microscope BZ9000 (Keyence).

Immunochemistry. For trichloroacetic acid (TCA) precipitation, 10 mL of *S. pombe* cell culture (containing ∼1 × 10^8 cells) was mixed with a 1:4 volume (2.5 mL) of ice-cold 100% TCA. The resulting mixture was centrifuged, and pellets were washed with 10% TCA, followed by cell disruption with glass beads in 10% TCA. After centrifugation at 8,000 rpm (Tomy, MX-301) for 10 min at 4 °C, washed precipitates were resuspended in SDS sample buffer containing 1 mM PMSF and boiled at 70 °C for 10 min. After centrifugation at 14,000 rpm (Tomy, MX-301) for 10 min, supernatants were loaded onto custom-made 3–8% gradient Tris-acetate gels (NuPAGE; Invitrogen). Antibodies against FLAG (Sigma), Rad21 (17, 29, 64), Cnd3 (33), tubulin (TAT1; a gift from Keith Gull, University of Oxford, Oxford), and Cdc2 (PSTAIR; a gift from Yoshitaka Nagahama, National Institute for Basic Biology, Okazaki, Japan) were employed as primary antibodies. Anti-mouse–HRP and anti-rabbit–HRP were used as secondary antibodies.

Mutational Analysis of Suppressors in Protein Structures. Atomic models of *S. pombe* cohesin and condensin (Fig. 4 *C*, *F*, and *I*) were generated from existing crystal structures of cohesin and condensin from other organisms using homology modeling (8, 69). Mmi1 mutations in Fig. 3*C* were mapped onto a crystal structure of *S. pombe* Mmi1 in complex with 11-mer RNA [Protein Data Bank (PDB) ID code 6FPX]. The following structures used in this study are from other organisms; therefore, structural analysis was based on protein sequence alignment results. SUMO-Hus5-Pli1 mutations in Fig. 1*D* were mapped onto a crystal structure of *Saccharomyces cerevisiae* E2-SUMO-Siz1/E3-SUMO-PCNA complex, based on protein sequence alignment results (PDB ID code 5JNE). Hrp1 mutations in Fig. 3*E* were mapped onto a structure of nucleosome–Chd1 complex (PDB ID code 5O9G). Wpl1 mutations in Fig. 6*B* were mapped onto the structure of the Wpl1 protein (PDB ID code 3ZIK). Cut14 and Cnd2 N-terminal mutations in *SI Appendix*, Fig. S3*D* were mapped onto the structure of the kleisin-N SMC interface in prokaryotic condensin (PDB ID code 3ZGX). Cut3 and Cnd2 C-terminal mutations in *SI Appendix*, Fig. S3*E* were mapped onto the structure of the kleisin-C SMC interface (PDB ID code 4I99). The Psc3 mutation in *SI Appendix*, Fig. S5*D* was mapped onto the structure of Psc3 bound to a fragment of the Rad21 kleisin subunit and DNA (PDB ID code 6H8Q). Sck1 mutations in *SI Appendix*, Fig. S8*E* were mapped onto the structure of SGK1 in complex with AMP-PNP (PDB ID code 2R5T). Ksg1 mutations in *SI Appendix*, Fig. S8*F* were mapped onto the structure of human PDK1 catalytic domain (PDB ID code 1H1W).

ACKNOWLEDGMENTS. We thank Dr. Man-Wah Tsang and Dr. Haifeng Zhang for their help in condensin SUMOylation detection by immunoblotting, Dr. Norihiko Nakazawa and Dr. Ryuta Kanai for technical support and valuable discussions, and Dr. Steven D. Aird for technical editing. Generous support from the Okinawa Institute of Science and Technology Graduate University is acknowledged.

1. Hayles J, Beach D, Durkacz B, Nurse P (1986) The fission yeast cell cycle control gene cdc2: Isolation of a sequence suc1 that suppresses cdc2 mutant function. *Mol Gen Genet* 202:291–293.
2. Oliver SG (1996) From DNA sequence to biological function. *Nature* 379:597–600.
3. van Leeuwen J, Pons C, Boone C, Andrews BJ (2017) Mechanisms of suppression: The wiring of genetic resilience. *BioEssays* 39:1700042.
4. van Leeuwen J, et al. (2016) Exploring genetic suppression interactions on a global scale. *Science* 354:aag0839.
5. Mitsuzawa H (1993) Responsiveness to exogenous cAMP of a Saccharomyces cerevisiae strain conferred by naturally occurring alleles of PDE1 and PDE2. *Genetics* 135: 321–326.
6. Wang L, Griffiths K, Jr, Zhang YH, Ivey FD, Hoffman CS (2005) Schizosaccharomyces pombe adenylate cyclase suppressor mutations suggest a role for cAMP phosphodiesterase regulation in feedback control of glucose/cAMP signaling. *Genetics* 171:1523–1533.
7. Xu X, Wang L, Yanagida M (2018) Whole-genome sequencing of suppressor DNA mixtures identifies pathways that compensate for chromosome segregation defects in *Schizosaccharomyces pombe*. *G3 (Bethesda)* 8:1031–1038.
8. Xu X, et al. (2018) Suppressor mutation analysis combined with 3D modeling explains cohesin's capacity to hold and release DNA. *Proc Natl Acad Sci USA* 115:E4833–E4842.
9. Hirano T, Mitchison TJ (1994) A heterodimeric coiled-coil protein required for mitotic chromosome condensation in vitro. *Cell* 79:449–458.
10. Strunnikov AV, Larionov VL, Koshland D (1993) SMC1: An essential yeast gene encoding a putative head-rod-tail protein is required for nuclear division and defines a new ubiquitous protein family. *J Cell Biol* 123:1635–1648.
11. Koshland D, Strunnikov A (1996) Mitotic chromosome condensation. *Annu Rev Cell Dev Biol* 12:305–333.
12. Saka Y, et al. (1994) Fission yeast cut3 and cut14, members of a ubiquitous protein family, are required for chromosome condensation and segregation in mitosis. *EMBO J* 13:4938–4952.
13. Strunnikov AV, Hogan E, Koshland D (1995) SMC2, a Saccharomyces cerevisiae gene essential for chromosome segregation and condensation, defines a subgroup within the SMC family. *Genes Dev* 9:587–599.
14. Hirano T, Kobayashi R, Hirano M (1997) Condensins, chromosome condensation protein complexes containing XCAP-C, XCAP-E and a Xenopus homolog of the Drosophila Barren protein. *Cell* 89:511–521.
15. Sutani T, et al. (1999) Fission yeast condensin complex: Essential roles of non-SMC subunits for condensation and Cdc2 phosphorylation of Cut3/SMC4. *Genes Dev* 13: 2271–2283.

16. Chao WC, et al. (2017) Structure of the cohesin loader Scc2. *Nat Commun* 8:13952.
17. Tomonaga T, et al. (2000) Characterization of fission yeast cohesin: Essential anaphase proteolysis of Rad21 phosphorylated in the S phase. *Genes Dev* 14:2757–2770.
18. Hirano T, Mitchison TJ, Swedlow JR (1995) The SMC family: From chromosome condensation to dosage compensation. *Curr Opin Cell Biol* 7:329–336.
19. Kimura K, Hirano T (1997) ATP-dependent positive supercoiling of DNA by 13S condensin: A biochemical implication for chromosome condensation. *Cell* 90:625–634.
20. Haering CH, Löwe J, Hochwagen A, Nasmyth K (2002) Molecular architecture of SMC proteins and the yeast cohesin complex. *Mol Cell* 9:773–788.
21. Bürmann F, et al. (2013) An asymmetric SMC-kleisin bridge in prokaryotic condensin. *Nat Struct Mol Biol* 20:371–379.
22. Diebold-Durand ML, et al. (2017) Structure of full-length SMC and rearrangements required for chromosome organization. *Molecular cell* 67:334–347.e5.
23. Gligoris TG, et al. (2014) Closing the cohesin ring: Structure and function of its Smc3-kleisin interface. *Science* 346:963–967.
24. Haering CH, et al. (2004) Structure and stability of cohesin's Smc1-kleisin interaction. *Mol Cell* 15:951–964.
25. Huis in 't Veld PJ, et al. (2014) Characterization of a DNA exit gate in the human cohesin ring. *Science* 346:968–972.
26. Kamada K, Su'etsugu M, Takada H, Miyata M, Hirano T (2017) Overall shapes of the SMC-ScpAB complex are determined by balance between constraint and relaxation of its structural parts. *Structure* 25:603–616.e4.
27. Funabiki H, et al. (1996) Cut2 proteolysis required for sister-chromatid seperation in fission yeast. *Nature* 381:438–441.
28. Funabiki H, et al. (1997) Fission yeast Cut2 required for anaphase has two destruction boxes. *EMBO J* 16:5977–5987.
29. Nagao K, Adachi Y, Yanagida M (2004) Separase-mediated cleavage of cohesin at interphase is required for DNA repair. *Nature* 430:1044–1048.
30. Uhlmann F, Lottspeich F, Nasmyth K (1999) Sister-chromatid separation at anaphase onset is promoted by cleavage of the cohesin subunit Scc1. *Nature* 400:37–42.
31. Uhlmann F, Wernic D, Poupart MA, Koonin EV, Nasmyth K (2000) Cleavage of cohesin by the CD clan protease separin triggers anaphase in yeast. *Cell* 103:375–386.
32. Xu X, Nakazawa N, Yanagida M (2015) Condensin HEAT subunits required for DNA repair, kinetochore/centromere function and ploidy maintenance in fission yeast. *PLoS One* 10:e0119347.
33. Aono N, Sutani T, Tomonaga T, Mochida S, Yanagida M (2002) Cnd2 has dual roles in mitotic condensation and interphase. *Nature* 417:197–202.
34. Xu X, Yanagida M (March 26, 2019) Isolation of fission yeast condensin temperature-sensitive mutants with single amino acid substitutions targeted to hinge domain. *G3 (Bethesda),* 10.1534/g3.119.400156.
35. Tatebayashi K, Kato J, Ikeda H (1998) Isolation of a Schizosaccharomyces pombe rad21ts mutant that is aberrant in chromosome segregation, microtubule function, DNA repair and sensitive to hydroxyurea: Possible involvement of Rad21 in ubiquitin-mediated proteolysis. *Genetics* 148:49–57.
36. Yuasa T, et al. (2004) An interactive gene network for securin-separase, condensin, cohesin, Dis1/Mtc1 and histones constructed by mass transformation. *Genes Cells* 9: 1069–1082.
37. Furuya K, Takahashi K, Yanagida M (1998) Faithful anaphase is ensured by Mis4, a sister chromatid cohesion molecule required in S phase and not destroyed in G1 phase. *Genes Dev* 12:3408–3418.
38. al-Khodairy F, Enoch T, Hagan IM, Carr AM (1995) The Schizosaccharomyces pombe hus5 gene encodes a ubiquitin conjugating enzyme required for normal mitosis. *J Cell Sci* 108:475–486.
39. Shayeghi M, Doe CL, Tavassoli M, Watts FZ (1997) Characterisation of Schizosaccharomyces pombe rad31, a UBA-related gene required for DNA damage tolerance. *Nucleic Acids Res* 25:1162–1169.
40. Tanaka K, et al. (1999) Characterization of a fission yeast SUMO-1 homologue, pmt3p, required for multiple nuclear events, including the control of telomere length and chromosome segregation. *Mol Cell Biol* 19:8660–8672.
41. Xhemalce B, Seeler JS, Thon G, Dejean A, Arcangioli B (2004) Role of the fission yeast SUMO E3 ligase Pli1p in centromere and telomere maintenance. *EMBO J* 23:3844–3853.
42. Dasso M (2008) Emerging roles of the SUMO pathway in mitosis. *Cell Div* 3:5.
43. Køhler JB, et al. (2015) Targeting of SUMO substrates to a Cdc48-Ufd1-Npl4 segregase and STUbL pathway in fission yeast. *Nat Commun* 6:8827.
44. Schleiffer A, et al. (2003) Kleisins: A superfamily of bacterial and eukaryotic SMC protein partners. *Mol Cell* 11:571–575.
45. Kschonsak M, et al. (2017) Structural basis for a safety-belt mechanism that anchors condensin to chromosomes. *Cell* 171:588–600.e24.
46. Doughty TW, Arsenault HE, Benanti JA (2016) Levels of Ycg1 limit condensin function during the cell cycle. *PLoS Genet* 12:e1006216.
47. Harigaya Y, et al. (2006) Selective elimination of messenger RNA prevents an incidence of untimely meiosis. *Nature* 442:45–50.
48. Sugiyama T, Sugioka-Sugiyama R (2011) Red1 promotes the elimination of meiosis-specific mRNAs in vegetatively growing fission yeast. *EMBO J* 30:1027–1039.
49. Yamashita A, Takayama T, Iwata R, Yamamoto M (2013) A novel factor Iss10 regulates Mmi1-mediated selective elimination of meiotic transcripts. *Nucleic Acids Res* 41: 9680–9687.
50. Krzyzanowski MK, Kozlowska E, Kozlowski P (2012) Identification and functional analysis of the erh1(+) gene encoding enhancer of rudimentary homolog from the fission yeast Schizosaccharomyces pombe. *PLoS One* 7:e49059.
51. Sugiyama T, et al. (2016) Enhancer of rudimentary cooperates with conserved RNA-processing factors to promote meiotic mRNA decay and facultative heterochromatin assembly. *Mol Cell* 61:747–759.
52. Weng MT, Luo J (2013) The enigmatic ERH protein: Its role in cell cycle, RNA splicing and cancer. *Protein Cell* 4:807–812.
53. Stowell JAW, et al. (2018) A low-complexity region in the YTH domain protein Mmi1 enhances RNA binding. *J Biol Chem* 293:9210–9222.
54. Farnung L, Vos SM, Wigge C, Cramer P (2017) Nucleosome-Chd1 structure and implications for chromatin remodelling. *Nature* 550:539–542.
55. Fischer T, et al. (2009) Diverse roles of HP1 proteins in heterochromatin assembly and functions in fission yeast. *Proc Natl Acad Sci USA* 106:8998–9003.
56. Motamedi MR, et al. (2008) HP1 proteins form distinct complexes and mediate heterochromatic gene silencing by nonoverlapping mechanisms. *Mol Cell* 32:778–790.
57. Krantz ID, et al. (2004) Cornelia de Lange syndrome is caused by mutations in NIPBL, the human homolog of Drosophila melanogaster Nipped-B. *Nat Genet* 36:631–635.
58. Tonkin ET, Wang TJ, Lisgo S, Bamshad MJ, Strachan T (2004) NIPBL, encoding a homolog of fungal Scc2-type sister chromatid cohesion proteins and fly Nipped-B, is mutated in Cornelia de Lange syndrome. *Nat Genet* 36:636–641.
59. Li Y, et al. (2018) Structural basis for Scc3-dependent cohesin recruitment to chromatin. *eLife* 7:e38356.
60. Murayama Y, Uhlmann F (2015) DNA entry into and exit out of the cohesin ring by an interlocking gate mechanism. *Cell* 163:1628–1640.
61. Ouyang Z, Yu H (2017) Releasing the cohesin ring: A rigid scaffold model for opening the DNA exit gate by Pds5 and Wapl. *BioEssays* 39:1600207.
62. Ouyang Z, et al. (2013) Structure of the human cohesin inhibitor Wapl. *Proc Natl Acad Sci USA* 110:11355–11360.
63. Chatterjee A, Zakian S, Hu XW, Singleton MR (2013) Structural insights into the regulation of cohesion establishment by Wpl1. *EMBO J* 32:677–687.
64. Adachi Y, Kokubu A, Ebe M, Nagao K, Yanagida M (2008) Cut1/separase-dependent roles of multiple phosphorylation of fission yeast cohesion subunit Rad21 in post-replicative damage repair and mitosis. *Cell Cycle* 7:765–776.
65. Shimanuki M, et al. (1993) Isolation and characterization of the fission yeast protein phosphatase gene ppe1+ involved in cell shape control and mitosis. *Mol Biol Cell* 4: 303–313.
66. Goshima G, Iwasaki O, Obuse C, Yanagida M (2003) The role of Ppe1/PP6 phosphatase for equal chromosome segregation in fission yeast kinetochore. *EMBO J* 22:2752–2763.
67. Zhao B, et al. (2007) Crystal structure of the kinase domain of serum and glucocorticoid-regulated kinase 1 in complex with AMP PNP. *Protein Sci* 16:2761–2769.
68. Biondi RM, et al. (2002) High resolution crystal structure of the human PDK1 catalytic domain defines the regulatory phosphopeptide docking site. *EMBO J* 21:4219–4228.
69. Akai Y, et al. (2014) ATPase-dependent auto-phosphorylation of the open condensin hinge diminishes DNA binding. *Open Biol* 4:140193.
70. Yanagida M (2009) Clearing the way for mitosis: Is cohesin a target? *Nat Rev Mol Cell Biol* 10:489–496.
71. Nakazawa N, et al. (2008) Dissection of the essential steps for condensin accumulation at kinetochores and rDNAs during fission yeast mitosis. *J Cell Biol* 180:1115–1131.
72. Nakazawa N, et al. (2015) RNA pol II transcript abundance controls condensin accumulation at mitotically up-regulated and heat-shock-inducible genes in fission yeast. *Genes Cells* 20:481–499.
73. Sutani T, et al. (2015) Condensin targets and reduces unwound DNA structures associated with transcription in mitotic chromosome condensation. *Nat Commun* 6: 7815.
74. Yong-Gonzales V, Hang LE, Castellucci F, Branzei D, Zhao X (2012) The Smc5-Smc6 complex regulates recombination at centromeric regions and affects kinetochore protein sumoylation during normal growth. *PLoS One* 7:e51540.
75. Skibbens RV (2019) Condensins and cohesins–One of these things is not like the other! *J Cell Sci* 132:jcs220491.
76. Hirano M, Anderson DE, Erickson HP, Hirano T (2001) Bimodal activation of SMC ATPase by intra- and inter-molecular interactions. *EMBO J* 20:3238–3250.
77. Hirano M, Hirano T (2002) Hinge-mediated dimerization of SMC protein is essential for its dynamic interaction with DNA. *EMBO J* 21:5733–5744.
78. Hirano M, Hirano T (2006) Opening closed arms: Long-distance activation of SMC ATPase by hinge-DNA interactions. *Mol Cell* 21:175–186.
79. Skibbens RV (2016) Of rings and rods: Regulating cohesin entrapment of DNA to generate intra- and intermolecular tethers. *PLoS Genet* 12:e1006337.
80. Liu Y, et al. (2016) ATP-dependent DNA binding, unwinding, and resection by the Mre11/Rad50 complex. *EMBO J* 35:743–758.
81. Rojowska A, et al. (2014) Structure of the Rad50 DNA double-strand break repair protein in complex with DNA. *EMBO J* 33:2847–2859.
82. Seifert FU, Lammens K, Stoehr G, Kessler B, Hopfner KP (2016) Structural mechanism of ATP-dependent DNA binding and DNA end bridging by eukaryotic Rad50. *EMBO J* 35:759–772.
83. Forsburg SL, Rhind N (2006) Basic methods for fission yeast. *Yeast* 23:173–183.
84. Hiraoka Y, Toda T, Yanagida M (1984) The NDA3 gene of fission yeast encodes beta-tubulin: A cold-sensitive nda3 mutation reversibly blocks spindle formation and chromosome movement in mitosis. *Cell* 39:349–358.
85. Moreno S, Hayles J, Nurse P (1989) Regulation of p34cdc2 protein kinase during mitosis. *Cell* 58:361–372.
86. Zhao Q, et al. (2014) GPS-SUMO: A tool for the prediction of sumoylation sites and SUMO-interaction motifs. *Nucleic Acids Res* 42:W325–W330.